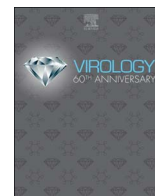




Since January 2020 Elsevier has created a COVID-19 resource centre with free information in English and Mandarin on the novel coronavirus COVID-19. The COVID-19 resource centre is hosted on Elsevier Connect, the company's public news and information website.

Elsevier hereby grants permission to make all its COVID-19-related research that is available on the COVID-19 resource centre - including this research content - immediately available in PubMed Central and other publicly funded repositories, such as the WHO COVID database with rights for unrestricted research re-use and analyses in any form or by any means with acknowledgement of the original source. These permissions are granted for free by Elsevier for as long as the COVID-19 resource centre remains active.



Nonstructural protein 9 residues 586 and 592 are critical sites in determining the replication efficiency and fatal virulence of the Chinese highly pathogenic porcine reproductive and respiratory syndrome virus

Lei Xu, Lei Zhou, Weifeng Sun, Pingping Zhang, Xinna Ge, Xin Guo, Jun Han, Hanchun Yang*

Key Laboratory of Animal Epidemiology of the Ministry of Agriculture, College of Veterinary Medicine and State Key Laboratory of Agrobiotechnology, China Agricultural University, Beijing 100193, People's Republic of China

ARTICLE INFO

Keywords:

Porcine reproductive and respiratory syndrome virus (PRRSV)
Highly pathogenic PRRSV (HP-PRRSV)
Nonstructural protein 9 (nsp9)
Mutant virus
Replication efficiency
Virulence

ABSTRACT

The highly pathogenic porcine reproductive and respiratory syndrome virus (HP-PRRSV) has caused huge economic losses to the swine industry in China. Understanding the molecular basis in relation to the virulence of HP-PRRSV is essential for effectively controlling clinical infection and disease. In the current study, we constructed and rescued a serial of mutant viruses in nsp9 and nsp10 based on the differential amino acid sites between HP-PRRSV JXwn06 and LP-PRRSV HB-1/3.9. The replication efficiency in pulmonary alveolar macrophages (PAMs) and the pathogenicity of the mutant viruses for piglets were analyzed. Our results showed that the mutation of Thr to Ala in 586 and Ser to Thr in 592 of nsp9 decreased the replication efficiency of HP-PRRSV in PAMs, and could attenuate its virulence for piglets, suggesting that the residues 586 and 592 of nsp9 are critical sites natively in determining the fatal virulence of the Chinese HP-PRRSV for piglets.

1. Introduction

Porcine reproductive and respiratory syndrome virus (PRRSV), a devastating pathogen for global swine industry, causes severe reproductive failures in sows and respiratory distress in growing pigs (Albina, 1997; Rossow, 1998). The virus remains a threat to pig production since it was first recognized in the early 1990s (Benfield et al., 1992; Wensvoort et al., 1991). PRRSV is an enveloped virus with a single positive-stranded genomic RNA, which is newly proposed to be classified into the genus *Porartevirus* of the family *Arteriviridae* in the order *Nidovirales*, together with lactate dehydrogenase-elevating virus (LDV) and rat arterivirus 1 (Kuhn et al., 2016; https://talk.ictvonline.org/ictv-reports/ictv_online_report/). PRRSV has two species (PRRSV1 and PRRSV2) (Kuhn et al., 2016), namely the European type (type 1) and North American type (type 2), based on genetic and antigenic differences (Allende et al., 1999; Mardassi et al., 1994; Meng et al., 1995; Murtaugh et al., 1995; Nelsen et al., 1999). The PRRSV genome is approximately 15 kb in size, and contains 12 known open reading frames (ORFs). The ORF1a and ORF1b situated in the 5'-proximal three quarters of the genome encode two large polypeptides, pp1a and pp1ab, which can be processed into 16 nonstructural proteins (nsp), including nsp1 α/β , nsp2-6, nsp7 α/β , nsp8-12, as well as nsp2TF and nsp2N (Fang et al., 2012; Fang and Snijder, 2010; Li et al., 2015; Mardassi et al.,

1995; Meulenber et al., 1995). The ORF2a, ORF2b, ORFs3-7, and ORF5a encode viral structural proteins (Johnson et al., 2011; Mardassi et al., 1995; Meulenber et al., 1995; van Nieuwstadt et al., 1996; Wu et al., 2001). The majority of PRRSV nsps have been shown to play important roles in viral replication, genomic transcription and the modulation of innate immune responses (Fang and Snijder, 2010; Yoo et al., 2010).

Tremendous molecular epidemiological data have shown that either type 1 or type 2 PRRSV exhibits broad genetic variation and diversified strains (Shi et al., 2010). The persistent evolution nature of PRRSV has led to the emergence of novel and variant strains with higher pathogenicity or virulence (Han et al., 2006; Karniychuk et al., 2010; Tian et al., 2007; Wang et al., 2015; Zhou et al., 2015). The Chinese highly pathogenic PRRSV (HP-PRRSV) with a unique hallmark of 30-amino acid deletion in the viral nsp2 emerged and prevailed in 2006 (Tian et al., 2007), causing colossal economic losses to the swine production (Zhou and Yang, 2010). A number of studies have provided essential evidence for understanding the pathogenesis of the Chinese HP-PRRSV (Han et al., 2017). HP-PRRSV infection is shown to display expanded tissue tropism and increased virus loads in a variety of organs (Hu et al., 2013; Li et al., 2012), and cause more severe lung injuries and histopathological changes (Han et al., 2014; Hu et al., 2013), and thymus atrophy, depletion of thymocytes, and apoptotic cell death of thymic

* Correspondence to: College of Veterinary Medicine, China Agricultural University, No. 2 Yuanmingyuan West Road, Haidian District, Beijing 100193, People's Republic of China.
E-mail address: yanghanchun1@cau.edu.cn (H. Yang).

epithelial cells (Guo et al., 2013; He et al., 2012; Li et al., 2014b). Importantly, much attention has been paid to the molecular basis in relation to its virulence. Our previous study indicated that the 30-amino acid deletion in its nsp2 is not related to the fatal virulence for piglets (Zhou et al., 2009). Subsequent works clearly revealed that the nsp9 and nsp10 together are closely related to the replication efficiency both *in vitro* and *in vivo*, and contribute to the fatal virulence of the Chinese HP-PRRSV (Li et al., 2014c). However, it remains unclear whether the Chinese HP-PRRSV shares the amino acid sites in nsp9 or/and nsp10 determining its fatal virulence.

In arterivirus, the nsp9 possesses RNA-dependent RNA polymerase (RdRp) activity, and the nsp10 contains metal binding region with RNA helicase activity, which are considered to be assembled into the replication and transcription complex (RTC), and to play a crucial role in virus replication (Beerens et al., 2007; van Dinten et al., 2000). In terms of the structural model of coronavirus nsp12 (Gorbalenya et al., 1989; Xu et al., 2003), the nsp9 of PRRSV is predicated to consist of at least two domains, an N-terminal domain with RdRp-associated nucleotidyltransferase (NiRAN) activity and a canonical RdRp occupying its C-terminal domain (Lehmann et al., 2015a). A conserved SDD motif and Asp residue within the RdRp domain of nsp9 are recognized to be critical for RNA polymerase activity and RNA synthesis (Lehmann et al., 2016; Snijder et al., 1990; Subissi et al., 2014). The nsp10 of arterivirus belongs to superfamily 1 helicase (HEL1), and its helicase activity domain has similar structure to a cellular helicase Usp1 that participates in nonsense-mediated mRNA decay pathway, implying that the nsp10 might also play a role in post-transcriptional quality control of viral RNA (Deng et al., 2014; Lehmann et al., 2015b). In the present study, we constructed a serial of mutant viruses with the mutated amino acid residues in the nsp9 and nsp10 of PRRSV by using reverse genetic approach, based on the differential amino acid sites in nsp9 and nsp10 between HP-PRRSV and low pathogenic PRRSV (LP-PRRSV), and analyzed the replication efficiency and pathogenicity of mutant viruses for piglets, in an attempt to identify the critical amino acids in relation to the fatal virulence in nsp9 or/and nsp10 of HP-PRRSV.

2. Materials and methods

2.1. Ethics statements

The animal experiments in this study were approved by the Laboratory Animal Ethical Committee of China Agricultural University with the license number (CAU20160828-2). All animal experiments were performed according to the Chinese Regulations of Laboratory Animals—The Guidelines for the Care of Laboratory Animals (Ministry of Science and Technology of People's Republic of China) and Laboratory Animal-Requirements of Environment and Housing Facilities (National Laboratory Animal Standardization Technical Committee).

2.2. Cells, infectious cDNA clones of PRRSV and viruses

MARC-145 cells (ATCC CRL-12231), a subclone of the African green monkey kidney epithelial cell line, were used for PRRSV propagation. The cells were cultured in Dulbecco's modified Eagle medium (DMEM) (Fisher Scientific, Waltham, MA), supplemented with 10% fetal bovine sera (FBS) (HyClone Laboratories Inc., South Logan, UT) at 37 °C under a humid 5% CO₂ atmosphere. Porcine pulmonary alveolar macrophages (PAMs) were prepared as previously described (Zhang et al., 2009), and used for growth efficiency analysis of the viruses. PAMs were maintained in RPMI 1640 medium (Fisher Scientific) supplemented with 10% FBS, 50 U/ml penicillin, 50 mg/ml streptomycin, at 37 °C under a humid 5% CO₂ atmosphere. The full-length infectious cDNA clones of HP-PRRSV JXwn06 and the chimeric infectious cDNA clones between JXwn06 and LP-PRRSV HB-1/3.9 were used in this study, including pWSK-RvJXwn, pWSK-RvJHn10, pWSK-RvJHn9n10, pWSK-

Table 1
Differential amino acid sites in nsp9 and nsp10 between PRRSV JXwn06 and HB-1/3.9.

Amino acid positions ^a	JXwn06 (nt/aa)	HB-1/3.9 (nt/aa)
nsp9		
427	GCC/Ala	ACC/Thr
586	ACC/Thr	GCC/Ala
592	TCA/Ser	ACA/Thr
609	GAC/Asp	GGC/Gly
nsp10		
11	GGG/Gly	ATG/Met
51	AGT/Ser	GGT/Gly
69	GAA/Glu	GGA/Gly
296	ATG/Met	GTG/Val
408	AGA/Arg	AAA/Lys

^a The positions are determined based on amino acid sequence of nsp9 and nsp10 of these two strains of PRRSV, respectively.

RvHJn9n10 and pWSK-RvHJn10, which were constructed previously in our laboratory (Li et al., 2014c; Zhou et al., 2009). For virus growth efficiency analysis and animal experiments, the rescued viruses (RvJXwn, RvJHn9n10, RvJHn10, RvHB-1/3.9, RvHJn9n10 and RvHJn10) conserved in our laboratory were utilized in this study (Li et al., 2014c; Zhou et al., 2009).

2.3. Construction of infectious cDNA clones with mutated sites in nsp9 and nsp10 of PRRSV and virus rescue

By aligning the amino acid sequences, totally nine different amino acid residues existed in nsp9, including nsp8 that is considered an N-terminal domain of nsp9 (Lunney et al., 2016), and nsp10 between the HP-PRRSV JXwn06 and LP-PRRSV HB-1/3.9 with an amino acid deletion in nsp9 that is not counted (Zhou et al., 2009). Of them, four amino acids located in the position 427, 586, 592 and 609 of nsp9, and five located in the position 11, 51, 69, 296 and 408 of nsp10 (Table 1). According to the strategies as previously described (Zhou et al., 2009), respective nucleotide mutation targeting the differential residues in the fragment C (containing nsp9- and nsp10-coding region) of infectious cDNA clones was conducted with the unique restriction enzymes *NheI* and *AscI* (New England Biolabs, Ipswich, MA). The plasmid Pjet1.2/blunt (Fisher Scientific) was used to construct the plasmid Pjet1.2-C, which was then inserted the fragment C. Then the target nucleotides were mutated in the plasmid by fast mutagenesis system (TransGen, Beijing, China). The mutant plasmids and the backbones of infectious cDNA clones were digested by the restriction enzymes *NheI* and *AscI*, and finally the mutated fragment C was inserted into the backbone to generate the full-length infectious cDNA clone with respective mutated site.

MARC-145 cells were transfected with the mutant full-length cDNA clone by Lipofectamine LTX (Fisher Scientific) and serially passaged for three times in MARC-145 cells. Then the rescued viruses were examined by indirect immunofluorescence assay (IFA) using the PRRSV N-specific monoclonal antibody (mAb) SDOW17 (Rural Technologies, Brookings, SD). The RNAs of third-passage rescued viruses were extracted, and amplified by RT-PCR, and the amplified fragment was sequenced to further confirm the mutated sites.

2.4. Animals and animal trials

Healthy, six-week old, landrace piglets were obtained from Beijing Center for SPF Swine Breeding & Management that is known to be free of PRRSV. All piglets were confirmed to be negative for PRRSV infection by commercial IDEXX ELISA kits and RT-PCR detection in our laboratory. The piglets were raised in the animal facilities at China Agricultural University (CAU).

The piglets were randomly divided into different groups based on the animal experiments design. The animals in each group (n = 5) were

Table 2
The list of rescued viruses with mutated respective amino acid sites.

Mutations	Parental viruses			
	RvJXwn	RvJHn10	RvJHn9n10	RvHJn10
A→T in 427 site of JX nsp ^a				HJn9n10-A427T
T→A in 586 site of JX nsp ^a	JXwn-T586A	JHn10-T586A		HJn9n10-T586A
S→T in 592 site of JX nsp ^a	JXwn-S592T	JHn10-S592T		HJn9n10-S592T
D→G in 609 site of JX nsp ^a				HJn9n10-D609G
G→M in 11 site of JX nsp ¹⁰ ^a				HJn9n10-G11M
S→G in 51 site of JX nsp ¹⁰				HJn9n10-S51G
E→G in 69 site of JX nsp ¹⁰				HJn9n10-E69G
M→V in 296 site of JX nsp ¹⁰				HJn9n10-M296V
R→K in 408 site of JX nsp ¹⁰				HJn9n10-R408K
T→A in 427 site of HB nsp ^b			JHn9n10-T427A	
A→T in 586 site of HB nsp ^b			JHn9n10-A586T	
T→S in 592 site of HB nsp ^b			JHn9n10-T592S	
G→D in 609 site of HB nsp ^b			JHn9n10-G609D	
M→G in 11 site of HB nsp ¹⁰ ^b			JHn9n10-M11G	
G→S in 51 site of HB nsp ¹⁰			JHn9n10-G51S	
G→E in 69 site of HB nsp ¹⁰			JHn9n10-G69E	
V→M in 296 site of HB nsp ¹⁰			JHn9n10-V296M	
K→R in 408 site of HB nsp ¹⁰			JHn9n10-K408R	
T→A in 586 and S→T in 592 site of JX nsp ⁹	JXwn-T586A/ S592T	JHn10-T586A/ S592T		
A→T in 427 and D→G in 609 site of JX nsp ⁹	JXwn-A427T/ D609G	JHn10-A427T/ D609G		
A→T in 586 and T→S in 592 site of HB nsp ⁹				HJn10-A586T/ T592S

The replication efficiency in PAMs of rescued viruses based on RvJHn9n10 and RvHJn9n10 were analyzed.
The replication efficiency in PAMs and the pathogenicity of rescued viruses based on RvJXwn and RvJHn10 were analyzed.
The pathogenicity of rescued virus based on RvHJn10 was analyzed.

^a JX nsp⁹/nsp¹⁰ represent nsp⁹ and nsp¹⁰ of JXwn06.
^b HB nsp⁹/nsp¹⁰ represent nsp⁹ and nsp¹⁰ of HB-1/3.9.

separately housed in different isolation rooms. Each piglet in each infection group was administered intranasally with 2 ml of respective virus (RvJXwn, JXwn-T586A, JXwn-S592T, JXwn-T586A/S592T, JXwn-A427T/D609G, RvJHn10, JHn10-T586A, JHn10-S592T, JHn10-T586A/S592T, JHn10-A427T/D609G, RvHJn10 and HJn10-A586T/T592S) of passage 3rd containing 10^5 TCID₅₀/ml. Each piglet in the control group received the same dose of MARC-145 cell culture supernatant. All the survived piglets were euthanized and necropsied on day 21 post-inoculation (dpi). Clinical examinations were performed and recorded daily. The average daily weight gain (ADG) was calculated by weighting the piglets at 7, 14 and 21 dpi, respectively.

2.5. The growth kinetics of rescued viruses in PAMs

Primary PAMs were infected with respective virus at a multiplicity of infection (MOI) of 0.1. The cell cultures were collected at 12 h, 24 h, 36 h, 48 h, 60 h and 72 h post-infection (pi) and the virus titers were determined using a microtitration infectivity assay, as previously described (Li et al., 2014c).

2.6. Quantification of PRRSV nsp9 gene by real-time PCR

Primary PAMs were infected with respective virus at a MOI of 1. The PAMs were collected prior to infection and at 12 h pi, and total RNA was extracted from the cells using TRIZOL Reagent according to the manufacturer's instructions (Fisher Scientific). 200 ng of RNAs were used for further RT-PCR. Real-time PCR was carried out using the SYBRGreen (ABI) on an ABI 7500 Fast Real Time PCR system (Life Technologies, Grand Island, NY). The primers used for detecting the copy numbers of PRRSV nsp9 gene were designed as previously described (Spear and Faaberg, 2015). Eight serial dilutions of plasmid with the copy number from 10^1 to 10^8 copies/ μ l served as template to run reaction on the ABI 7500 quantitative PCR machine to generate a standard curve. Cycling parameters used for all the reactions were as follows: 50 °C for 2 min; 95 °C for 2 min; and 40 cycles of 95 °C for 15 s, 60 °C for 60 s. Data collection was performed during the 60 °C elongation step. The standard curve was automatically generated and the numbers of nsp9 gene copy were calculated with the 7500 System SDS software (Applied Biosystems, Foster City, CA).

2.7. Microscopic pathological changes and immunohistochemistry (IHC) examinations

Microscopic pathological changes and IHC examinations for lung of each piglet were performed as previously described (Halbur et al., 1995, 1996). Briefly, lung tissue samples were taken, and fixed with 4% paraformaldehyde solution at room temperature for 48 h and then processed by conventional histopathological procedures. Two sections for each sample were prepared. One section was stained with hematoxylin and eosin (H&E) for microscopic pathological change examination, and another was stained with the mAb specific for PRRSV N protein (SDOW17) at 1:1000 dilutions for IHC examination of PRRSV antigen. The scores of lung microscopic lesions were blindly evaluated from 0 to 4, which accounted for the distribution and severity of interstitial pneumonia. The IHC scores of PRRSV antigen were conducted through a range score of 0–4 for evaluating the numbers of PRRSV-positive cells.

2.8. Viremia analysis

Serum samples of animals were collected at 0, 3, 5, 7, 10, 14 and 21 dpi to analyze the viral loads in the sera of the inoculated animals using a microtitration infectivity assay.

2.9. Statistical analysis

The significant differences were analyzed using a one-way or two-way RM ANOVA in the GraphPad Prism (version 5.0) software. A nonparametric test was employed to determine the significant difference in microscopic lung lesion scores and immunohistochemistry scores. Differences were considered statistically significant at a *p* value of < 0.05.

3. Results

3.1. The residues in the position 586 and 592 of nsp9 determined the replication efficiency of HP-PRRSV in PAMs

To screen for the potential amino acid sites affecting the replication efficiency of PRRSV, we used the chimeric full-length cDNA clones (pWSK-RvJHn9n10 and pWSK-RvHJn9n10), and constructed a serial of full-length cDNA clones with mutated differential amino acid sites in nsp9 and nsp10 between JXwn06 and HB-1/3.9. Totally, 18 viruses with a single residue mutation were rescued (Table 2). The replication efficiencies of these mutated viruses in PAMs were examined and compared by drawing growth curves, together with the parental viruses (RvJXwn, RvHB-1/3.9, RvJHn9n10 and RvHJn9n10). As shown in Fig. 1A, compared with the parental virus RvHB-1/3.9, the RvHJn9n10 with swapping nsp9- and nsp10-coding regions of JXwn06 had an increased replication efficiency in PAMs. While the HJn9n10-T586A with the mutation of Thr to Ala in 586 of nsp9 had lower titers than RvHJn9n10, with significant differences at 36 h and 48 h pi (*p* < 0.01); the HJn9n10-S592T with the mutation of Ser to Thr in 592 of nsp9 also showed the decreased titers, with a similar level to RvHB-1/3.9, and its titers were significantly lower than RvHJn9n10 at 36 h (*p* < 0.01) and 48 h pi (*p* < 0.05). The viruses with other mutations in nsp9 and nsp10 showed similar growth kinetics to the RvHJn9n10 (Fig. 1B). On other hand, we measured the growth kinetics of mutant viruses based on RvJHn9n10 with swapping nsp9- and nsp10-coding regions of HB-1/3.9. The results showed that RvJHn9n10 had a decreased replication efficiency than RvJXwn, but the viruses with mutated differential amino acid sites did not exhibit an increased growth efficiency than RvJHn9n10, even the viruses with the mutation of Ala to Thr in 586 and Thr to Ser in 592 of nsp9 (JHn9n10-A586T and JHn9n10-T592S) had slightly decreased titers (Fig. 1C and D). Obviously, these data indicate that it is insufficient to increase the replication efficiency of the chimeric PRRSV RvJHn9n10 by mutating only one amino acid.

To further confirm the influence of the two residues (586 and 592 in nsp9) on PRRSV replication, we used the full-length cDNA clone (pWSK-RvJXwn) of JXwn06 and constructed a serial of full-length cDNA clones with mutated differential amino acid sites in nsp9 and rescued the viruses (JXwn-T586A, JXwn-S592T, JXwn-T586A/S592T, JXwn-A427T/D609G) (Table 2). Meanwhile, considering that the nsp10 of HP-PRRSV also plays a role in its fatal virulence for piglets (Li et al., 2014c), we used the chimeric full-length infectious cDNA clone pWSK-RvJHn10 as backbone and mutated the corresponding amino acid sites, and rescued the viruses (JHn10-T586A, JHn10-S592T, JHn10-T586A/S592T and JHn10-A427T/D609G) (Table 2). Firstly, we evaluated the replication efficiency of these mutant viruses and their parental viruses in PAMs. As shown in Fig. 2A, the viruses with the mutation of Thr to Ala in 586 or Ser to Thr in 592 or both had lower titers than the parental virus RvJXwn, with significant difference at 24 h pi (*p* < 0.05), and delayed peak. While the viruses with the mutation of other two residues together showed no change of the replication efficiency. Similar data were obtained in the mutant viruses based on pWSK-RvJHn10. The titers of the viruses with the mutation of Thr to Ala in 586 or Ser to Thr in 592 or both decreased and their titer peaks delayed, while the viruses with the mutation of other two residues together had no significant differences in viral titers, compared with RvJHn10 (Fig. 2B).

Moreover, PAMs were infected with respective virus at a MOI of 1,

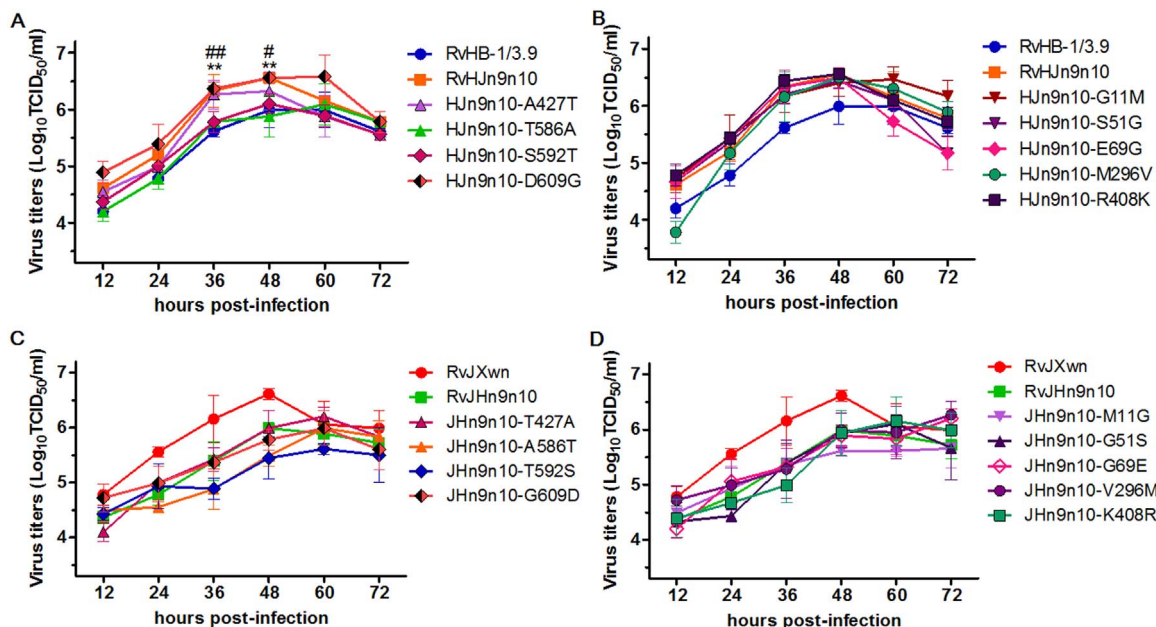


Fig. 1. The growth kinetics of the rescued viruses in PAMs. (A) and (B) The growth kinetics of the rescued viruses with the mutation of differential amino acid sites in nsp9 and nsp10 based on the infectious cDNA clone of RvHJn9n10. Asterisk (*) indicates a significant difference in the virus titers between RvHJn9n10 and HJn9n10-T586A (** $p < 0.01$). Pound (#) shows a significant difference in the virus titers between RvHJn9n10 and HJn9n10-S592T (# $p < 0.05$; ## $p < 0.01$). (C) and (D) The growth kinetics of the rescued viruses with the mutation of differential amino acid sites in nsp9 and nsp10 based on the infectious cDNA clone of RvJXwn. The data are shown as means \pm SD of three independent experiments.

and the copy numbers of nsp9 gene for the viruses were detected in order to evaluate the RNA synthesis efficiency by real-time PCR. As shown in Fig. 2C, the copy numbers of nsp9 gene of all viruses had a similar level at 0 h pi, while at 12 h pi, the average copy numbers of JXwn-T586A, JXwn-S592T and JXwn-T586A/S592T reached $7.16 \log_{10}/\mu\text{l}$, $7.46 \log_{10}/\mu\text{l}$, and $6.92 \log_{10}/\mu\text{l}$, respectively, which were remarkable lower than that of RvJXwn ($7.74 \log_{10}/\mu\text{l}$) ($p < 0.01$ or 0.001), in addition to the JXwn-A427T/D609G with a similar level to

RvJXwn. The RNA synthesis efficiency of the mutant viruses based on pWSK-RnJHn10 was also measured. The mutant viruses (JHn10-T586A, JHn10-S592T and JHn10-T586A/S592T), had the nsp9 copy numbers of $7.31 \log_{10}/\mu\text{l}$, $7.23 \log_{10}/\mu\text{l}$, and $6.95 \log_{10}/\mu\text{l}$, respectively, which were significantly lower than that of RvJHn10 ($7.75 \log_{10}/\mu\text{l}$) ($p < 0.001$), while the virus JHn10-A427T/D609G showed no statistically significant differences in nsp9 copy numbers with RvJHn10 (Fig. 2D).

Taken together, the above results indicated that the mutations of the

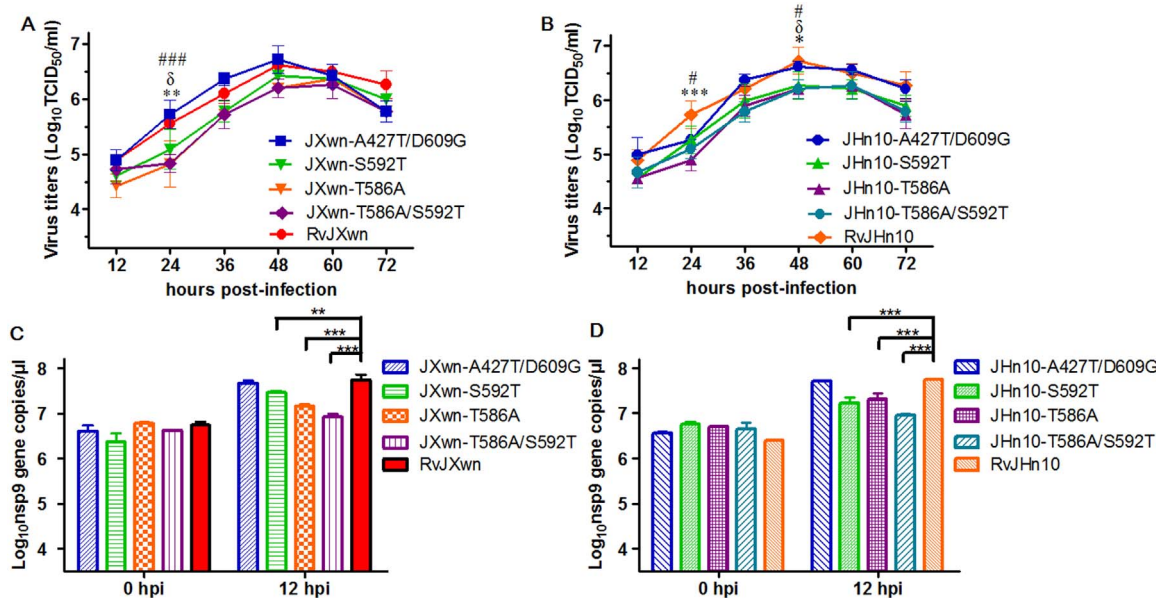


Fig. 2. The growth kinetics and viral RNA synthesis efficiency of the rescued viruses in PAMs. (A) The growth kinetics of the rescued viruses with the mutated differential amino acid sites in nsp9 based on the infectious cDNA clone of RvJXwn. Asterisk (*) indicates a significant difference in the virus titers between RvJXwn and JXwn-T586A (** $p < 0.01$). Delta (δ) indicates a significant difference in the virus titers between RvJXwn and JXwn-S592T ($\delta p < 0.05$). Pound (#) indicates a significant difference in the virus titers between RvJXwn and JXwn-T586A/S592T (### $p < 0.001$). (B) The growth kinetics of the rescued viruses with the mutated differential amino acid sites in nsp9 based on the infectious cDNA clone of RvJHn10. Asterisk (*) indicates a significant difference in the virus titers between RvJHn10 and JHn10-T586A (* $p < 0.05$; *** $p < 0.001$). Delta (δ) indicates a significant difference in the virus titers between RvJHn10 and JHn10-S592T ($\delta p < 0.05$). Pound (#) indicates a significant difference in the virus titers between RvJHn10 and JHn10-T586A/S592T (# $p < 0.05$). (C) and (D) The copy numbers of nsp9 gene of the rescued viruses with the mutated differential amino acid sites in nsp9 based on the infectious cDNA clone of RvJXwn and RvJHn10 at 0 and 12 hpi (** $p < 0.01$; *** $p < 0.001$). The data are shown as means \pm SD of three independent experiments.

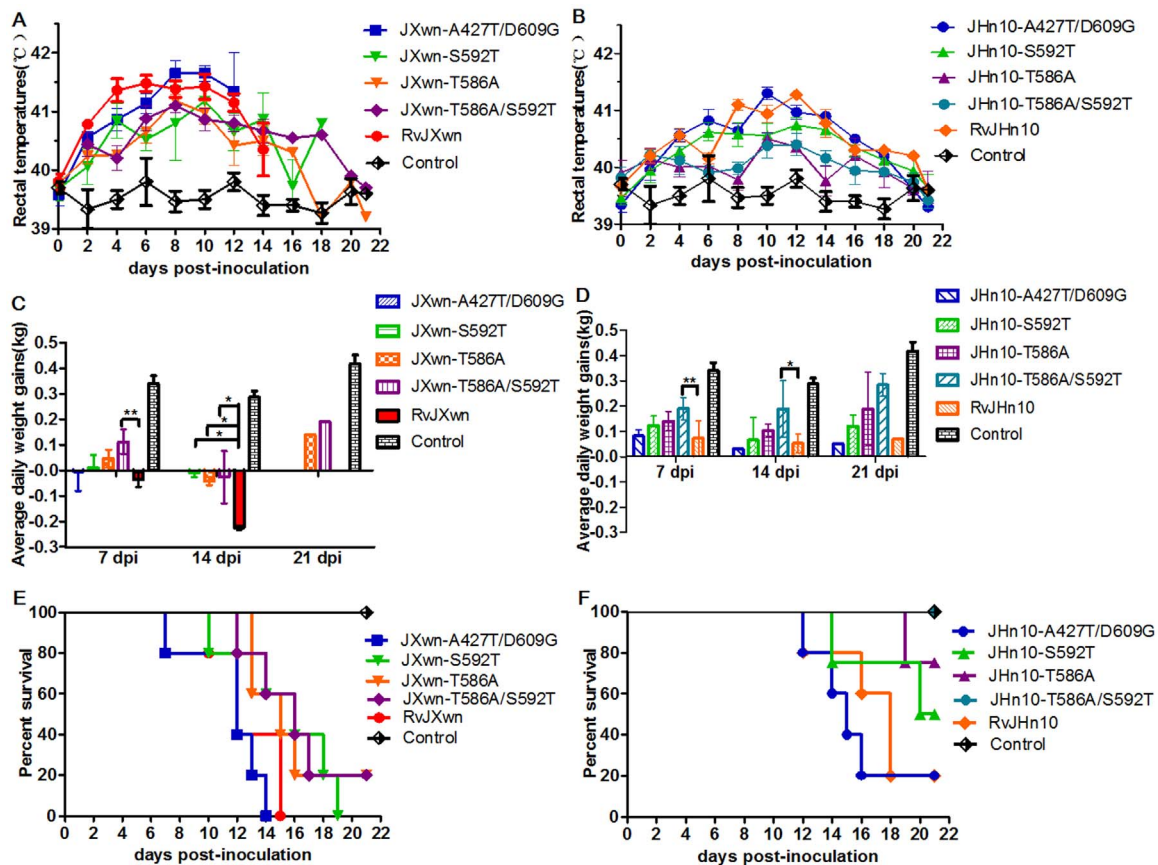


Fig. 3. The clinical responses and survive curves of piglets inoculated with the rescued viruses. The rectal temperatures, average daily weight gain (ADG) and survive curves of piglets inoculated with the rescued viruses based on the infectious cDNA clone of RvJXwn (A, C and E) or the infectious cDNA clone of RvJHn10 (B, D and F). The data are shown as means \pm SD (error bars) (* $p < 0.05$; ** $p < 0.01$).

residues 586 and 592 in nsp9 decreased the replication efficiency of HP-PRRSV in PAMs, while the mutations of the residues 427 and 609 in nsp9 did not, suggesting that the residues 586 and 592 in nsp9 contribute to the replication efficiency of HP-PRRSV.

3.2. Mutation of Thr to Ala in 586 and Ser to Thr in 592 of nsp9 attenuated the virulence of HP-PRRSV for piglets

The pathogenicity of the mutant viruses based on pWSK-RvJXwn and pWSK-RvJHn10 for piglets was analyzed. The piglets were inoculated with respective virus, and rectal temperatures of the inoculated piglets were daily recorded. JXwn-A427T/D609G-infected piglets displayed a similar temperature reaction to RvJXwn-infected piglets which reached the highest temperature (41.5 °C) and maintained above 41 °C from 4 to 12 dpi, while the piglets inoculated with the viruses with the mutation of Thr to Ala in 586 and Ser to Thr in 592 of nsp9 or both had a slow rising of body temperature, with the highest temperature of 41.2 °C and short lasting of above 41 °C (Fig. 3A). JHn10-A427T/D609G-infected piglets presented a similar temperature reaction to RvJHn10-infected group with the highest temperature (41.3 °C) and hovered above 41 °C from 8 to 14 dpi, while the piglets inoculated with the viruses with the mutation of Thr to Ala in 586 and Ser to Thr in 592 of nsp9 or both had a body temperature of less 41 °C (Fig. 3B).

The ADG of each group in animal trials was calculated. As shown in Fig. 3C, at the first week post-inoculation, the ADG of piglets inoculated with JXwn-T586A, JXwn-S592T, or JXwn-T586A/S592T was higher than that of RvJXwn-inoculated group, with a significant difference between JXwn-T586A/S592T- and RvJXwn-inoculated group ($p < 0.01$). From 7–14 dpi, the ADG of all the piglets inoculated with the

viruses reduced and the loss of ADG in RvJXwn-inoculated group was much larger ($p < 0.05$) than those in JXwn-T586A-, JXwn-S592T-, and JXwn-T586A/S592T-inoculated groups. While no significant differences in ADG were recorded between JXwn-A427T/D609G- and RvJXwn-inoculated groups. The similar data were observed in piglets inoculated with the mutant viruses based on pWSK-RvJHn10. Compared with RvJHn10-inoculated group, the ADG of JHn10-T586A-, JHn10-S592T- and JHn10-T586A/S592T-inoculated groups was higher, with significant differences in JHn10-T586A/S592T-inoculated group at 7 ($p < 0.01$) and 14 dpi ($p < 0.05$) (Fig. 3D).

The deaths of the piglets in each group were recorded. As shown in Fig. 3E, compared with RvJXwn-inoculated group with 5/5 mortality, JXwn-T586A-inoculated piglets began to die at 13 dpi and finally one piglet survived (4/5 mortality); all the piglets in JXwn-S592T-inoculated group died (5/5 mortality), but the survival time was prolonged; the survival time of JXwn-T586A/S592T-inoculated group was obviously prolonged and at last one piglet survived (4/5 mortality); JXwn-A427T/D609G-infected piglets showed no differences with RvJXwn-infected piglets in survival time and mortality. The survival rates of the piglets inoculated with the mutant viruses based on pWSK-RvJHn10 were shown in Fig. 3F. Compared with RvJHn10-infected group (4/5 mortality), only one piglet in JHn10-T586A-infected group died at 19 dpi (1/5 mortality); two piglets in JHn10-S592T-infected group died at 14 dpi and 20 dpi (2/5 mortality), respectively; all piglets in JHn10-T586A/S592T-inoculated group survived (0/5 mortality); while JHn10-A427T/D609G-infected group showed similar survival time and same mortality (4/5) with RvJHn10-infected group.

As a whole, the mutation of the residue 586 or 592 and the both in nsp9 of RvJXwn06 or RvJHn10 resulted in the alleviated temperature reaction, increased ADG and decreased mortality of the inoculated pigs,

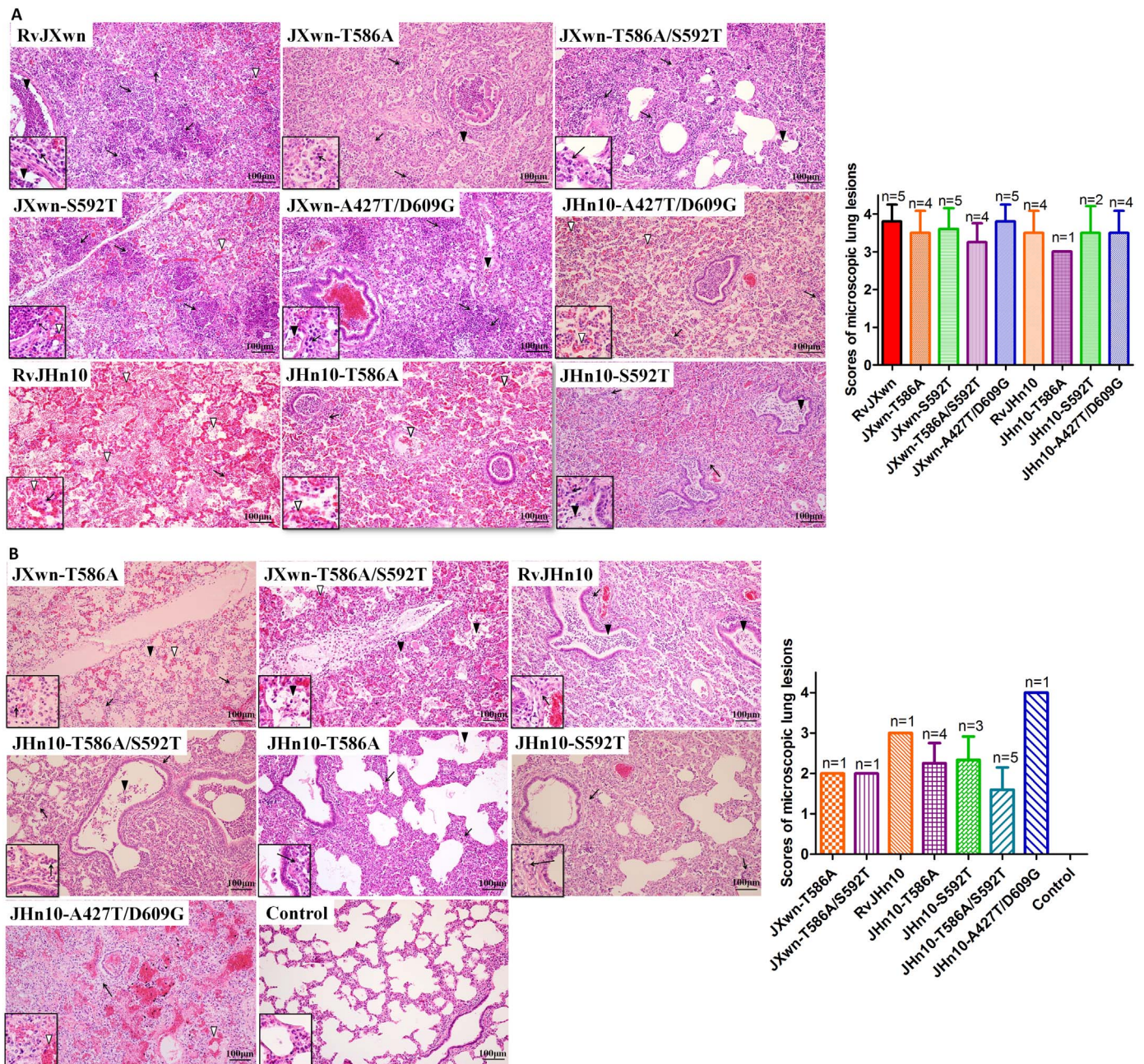


Fig. 4. Microscopic lung lesions of piglets inoculated with the rescued viruses. Shown are the representative microscopic lung lesions and the microscopic lesion scores by staining with hematoxylin and eosin (H&E) from dead piglets during the experiment (A) and from euthanized piglets by the termination of experiment (B) in each group. Solid arrow manifests infiltration of inflammatory cells or the thickening interlobular septal within alveolar septa, and alveolar spaces. Solid triangle indicates necrotic debris and exfoliated epithelial cells infiltrate. Triangle indicates hemorrhage in the bronchiole.

while the mutation of the residue 427 and 609 in nsp9 did not.

The lung microscopic lesions of the inoculated piglets were examined. The lung microscopic lesions of dead piglets post-inoculation and euthanized piglets at the termination of trials were shown in Fig. 4A and B, respectively. All the lungs of dead piglets in the inoculated groups exhibited severe histopathological changes with higher histopathological scores, including large amounts of inflammatory cells and fibrin exudation of the alveolar and bronchioles spaces, necrotic debris and hemorrhage, and the thickened interlobular septal and the destroyed lung structure (Fig. 4A). The euthanized piglets in JXwn-T586A- and JXwn-T586A/S592T-inoculated groups displayed moderate histopathological lesions (Fig. 4B). Compared with RvJHn10-inoculated piglets, the piglets inoculated with the mutant viruses showed the alleviated lung lesions with less inflammatory cells and fibrin exudation,

and lower histopathological scores, and the piglets in JHn10-A427T/D609G-inoculated group exhibited no differences in lung lesions with RvJHn10-inoculated piglets. No microscopic lesions were observed in the lungs of control piglets which survived until the trial termination. These results showed that the mutation of the residue 586 or both the residue 586 and 592 in nsp9 of RvJXwn06 or RvJHn10 alleviated the lung lesions of the survived pigs.

The virus loads in the sera of inoculated piglets were examined using a microtitration assay. The data showed that the virus titers in sera of piglets infected with JXwn-T586A, JXwn-T586A/S592T were lower than those of RvJXwn-infected group with significant differences at 3, 5, 10 dpi ($p < 0.01$, $p < 0.001$, $p < 0.05$), and the virus titers in JXwn-S592T-infected group were also slightly lower than those of RvJXwn-infected group, while JXwn-A427T/D609G-infected group had

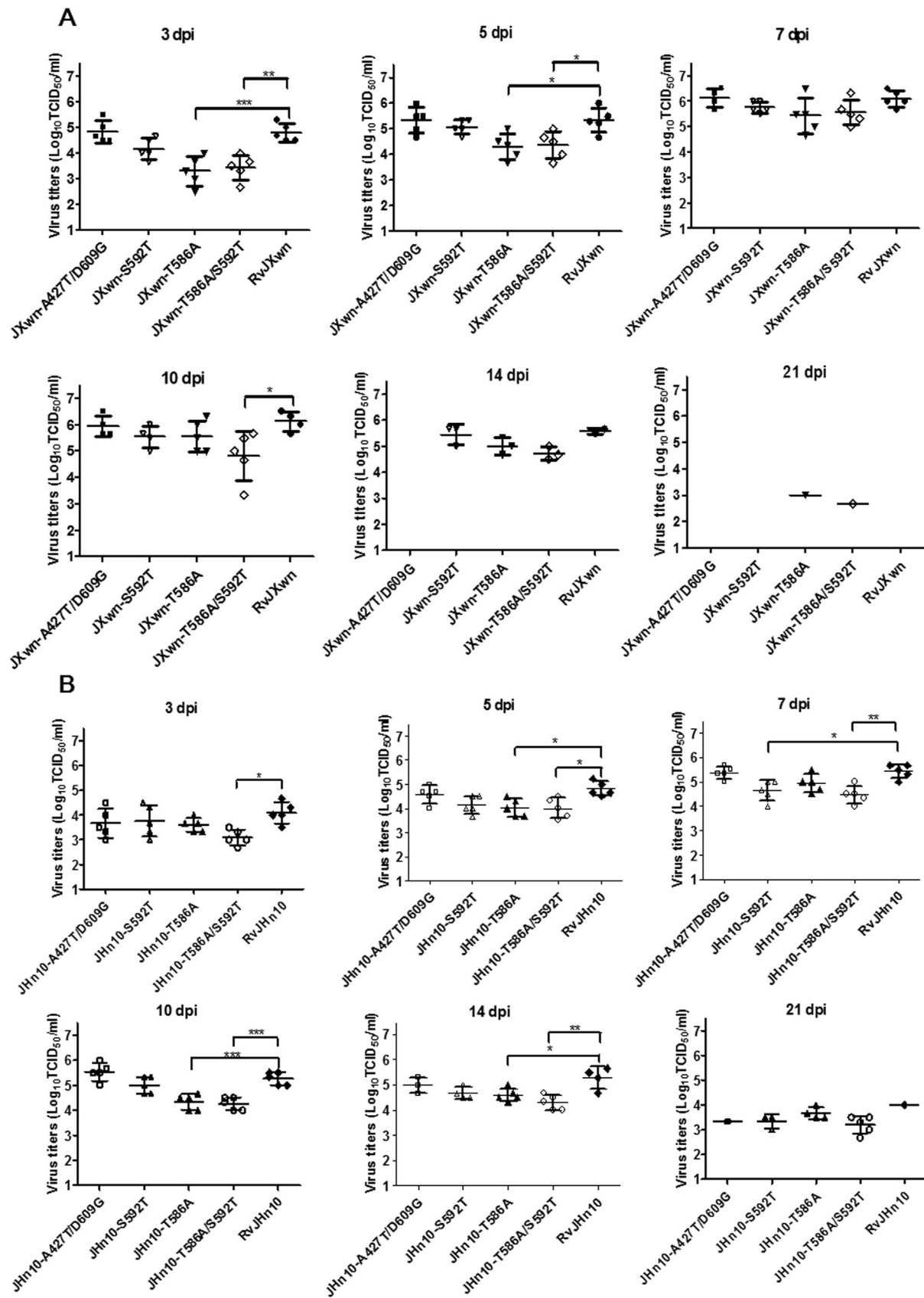


Fig. 5. Viral loads in the sera of piglets inoculated with the rescued viruses. Virus titers in the sera of piglets inoculated with rescued viruses based on the infectious cDNA clone of RvJXwn (A) or the infectious cDNA clone of RvJHn10 (B). The data are shown as means \pm SD (error bars) (* $p < 0.05$; ** $p < 0.01$; *** $p < 0.001$).

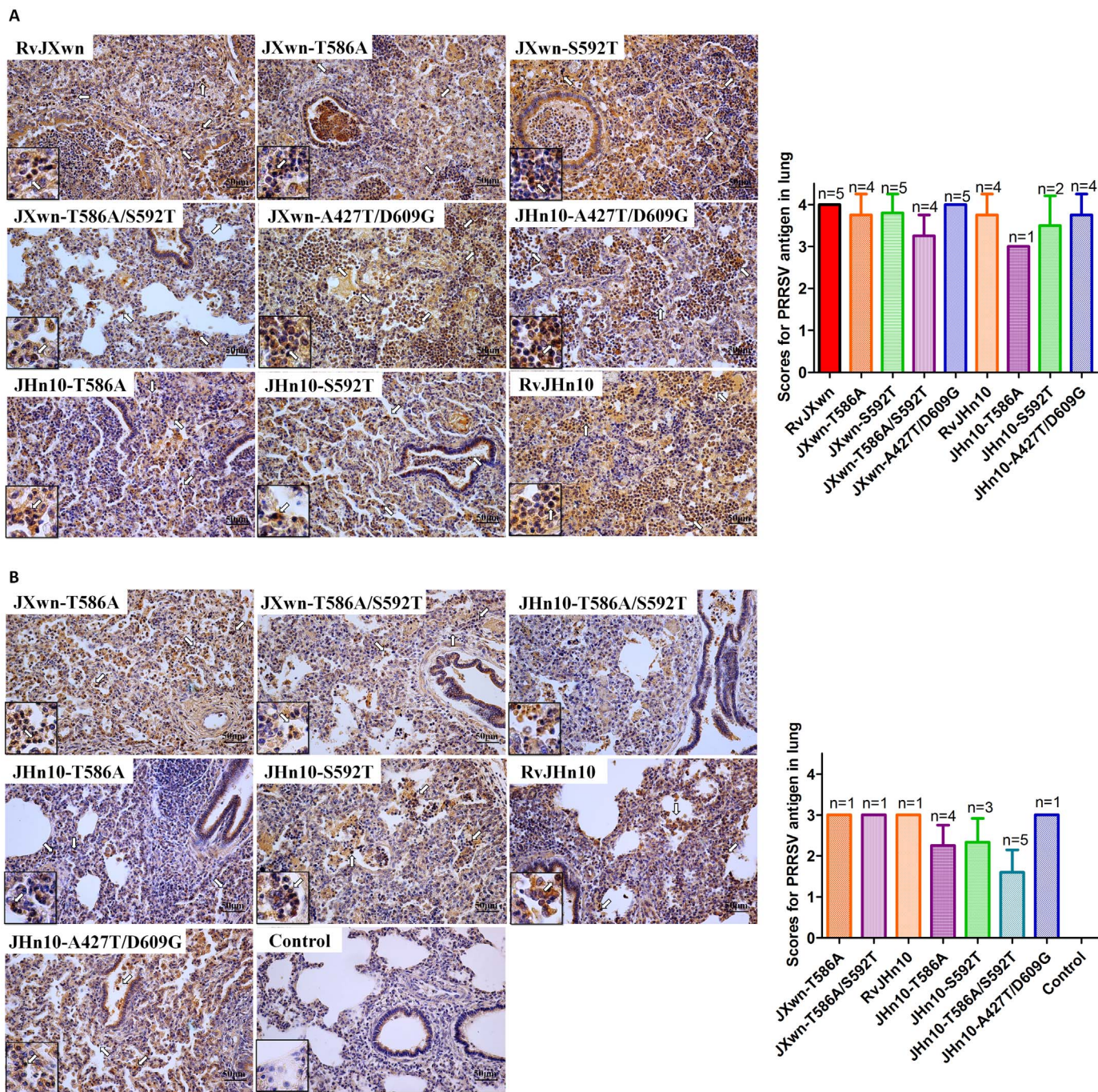


Fig. 6. Immunohistochemical examination for PRRSV antigen in lungs. Shown are the representative views of immunohistochemistry and mean scores of lungs of dead piglets during the experiment (A) and euthanized piglets by the termination of experiment (B) in each group. Solid arrow indicates positive signals in macrophages within or around alveolar septa and bronchiole.

no statistically significant differences in virus loads with RvJXwn-infected group (Fig. 5A). The virus titers in sera of the piglets infected with JHn10-T586A, JHn10-S592T, and JHn10-T586A/S592T were lower than those of RvJHn10-infected group with significant differences at some time points, and JHn10-T586A/S592T-infected piglets had the lowest virus loads, with significant differences at 3, 5, 7, 10, 14 dpi, while JHn10-A427T/D609G-infected piglets had no differences in virus loads with RvJHn10-infected group (Fig. 5B). The results indicated that the mutation of the residue 586 or 592 and the both in nsp9 of RvJXwn06 or RvJHn10 led to the declined virus load in the sera of the inoculated pigs.

Moreover, PRRSV antigen in lungs of the inoculated piglets was

examined by immunohistochemistry. The PRRSV-positive signals were distributed in all the lung section in dead piglets, and the scores of PRRSV antigen in lungs of the piglets inoculated with mutant viruses were lower than their respective parental viruses (Fig. 6A). For euthanized piglets, the PRRSV-positive signals in lungs of JHn10-T586A-, JHn10-S592T- and JHn10-T586A/S592T-inoculated piglets were less than those of RvJHn10-inoculated piglets, whereas JHn10-A427T/D609G-inoculated piglets showed no differences with RvJHn10-inoculated piglets (Fig. 6B). No PRRSV-positive signals were observed in lungs of control piglets.

Collectively, the above data revealed that the mutation of Thr to Ala in 586 and Ser to Thr in 592 of HP-PRRSV nsp9 alleviated the

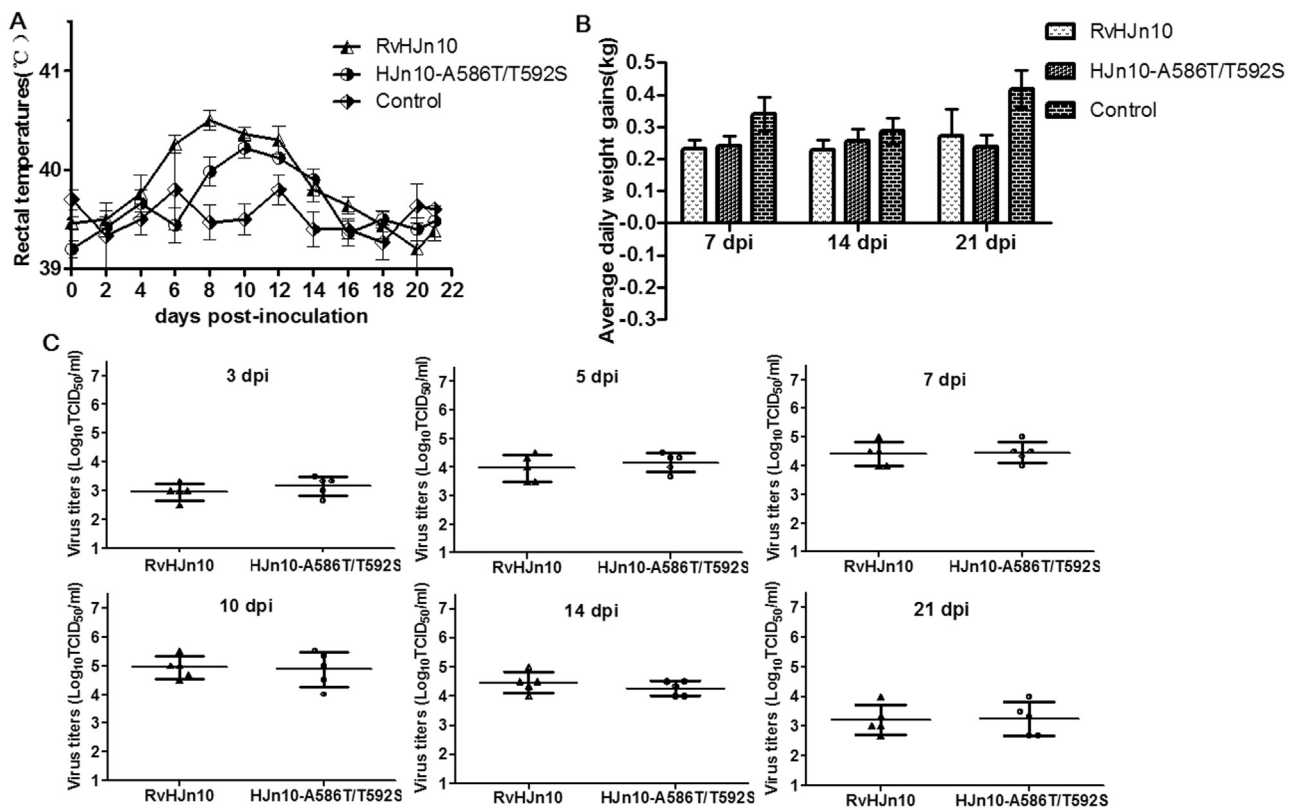


Fig. 7. The clinical outcomes of piglets inoculated with RvHJn10 and HJn10- A586T/T592S. Shown are the rectal temperatures (A), ADG (B) and virus titers in the sera (C) of piglets inoculated with the rescued viruses. The data are shown as means \pm SD (error bars).

temperature reaction and lung lesions of the infected piglets, and declined the replication efficiency of HP-PRRSV *in vivo*, and delayed the death time of the infected piglets, and resulted in the decreased mortality of piglets, suggesting that the mutation of these two residues in nsp9 of HP-PRRSV attenuates its virulence for piglets.

3.3. Mutation of the residues in 586 and 592 in nsp9 of LP-PRRSV did not enhance its pathogenicity for piglets

To address whether the mutation of amino acid sites in 586 and 592 of LP-PRRSV nsp9 enhances its pathogenicity for piglets, we performed the mutation of Ala to Thr in 586 and Thr to Ser in 592 in nsp9 of HB-1/3.9 using another chimeric full-length infectious clone pWSK-RvHJn10 and rescued the mutant virus (Table 2). Compared with RvHJn10-infected group, the piglets infected with HJn10-A586T/T592S showed no differences in body temperature reaction, with the highest temperatures of 40.2 °C (Fig. 7A), ADG (Fig. 7B), and virus loads in sera (Fig. 7C). Similar to RvHJn10, HJn10-A586T/T592S infection induced mild inflammatory reaction with low scores of microscopic lung lesions (Fig. 8A), and all the piglets survived during the whole period of experiments. Meanwhile the viral titers in sera of HJn10-A586T/T592S-inoculated piglets were lower and only a fewer PRRSV-positive signals distributed in lung (Fig. 8B). These results indicated that the mutation of the residue 586 or 592 and the both in nsp9 of RvHJn10 could not impact its pathogenicity for piglets, suggesting that the mutation of the two residues in nsp9 did not enhance the pathogenicity of LP-PRRSV for piglets.

4. Discussion

Chinese swine industry has been experiencing the damage of PRRSV for over two decades, and this situation has become even worse since HP-PRRSV emerged in 2006 (Han et al., 2017). Despite numerous

efforts on HP-PRRSV pathogenesis and antiviral immunity investigation for several years, to effectively control the clinical diseases caused by this virus remains a great challenge for the Chinese pig production. As a consequence, it is essential to find out the pathogenesis of HP-PRRSV. In our previous work, we utilized a HP-PRRSV strain JXwn06 and a LP-PRRSV strain HB-1/3.9 with genetic similarity to HP-PRRSV and swapped different viral coding regions by infectious cDNA clones, and clearly demonstrated that the nsp9 and nsp10 together were related to viral replication efficiency of HP-PRRSV *in vivo* and *in vitro*, contributing its fatal virulence for piglets (Li et al., 2014c). To further dissect the molecular basis of HP-PRRSV virulence, we screened for the critical amino acids in relation to the fatal virulence of HP-PRRSV in nsp9 and nsp10 in the current study.

As well known, many viruses can strengthen their pathogenicity by increasing viral replication efficiency (Brault et al., 2007; Hanley et al., 2002; Watanabe et al., 2009). Similar findings have been documented on PRRSV. In comparison to LP-PRRSV HB-1/3.9, HP-PRRSV JXwn06 exhibits stronger replication efficiency *in vivo* and *in vitro* (Zhou et al., 2009). The PRRSV Lena, a strain belonging to the subtype 3 of genotype 1, shares an increased virulence and higher replication efficiency (Karniychuk et al., 2010). Li et al. analyzed the replication efficiency differences of the chimeric viruses (RvJHn9n10 and RvHJn9n10) generated by swapping nsp9- and nsp10-coding region of LP-PRRSV HB-1/3.9 and HP-PRRSV JXwn06 and determined that the nsp9- and nsp10-coding regions together are closely related to the replication efficiency of the Chinese HP-PRRSV *in vitro* and *in vivo* (Li et al., 2014c). Moreover, the changes of replication efficiency were more significant in PAMs than in MARC-145 cells. Thus, we performed the mutation in nsp9 and nsp10 using the chimeric full-length infectious clones of RvJHn9n10 and RvHJn9n10 based on the differential amino acid sites between HP-PRRSV JXwn06 and LP-PRRSV HB-1/3.9. Considering that PAMs are the target cells of PRRSV, we evaluated the growth kinetics of all the rescued mutant viruses in PAMs instead of MARC-145 cells in the

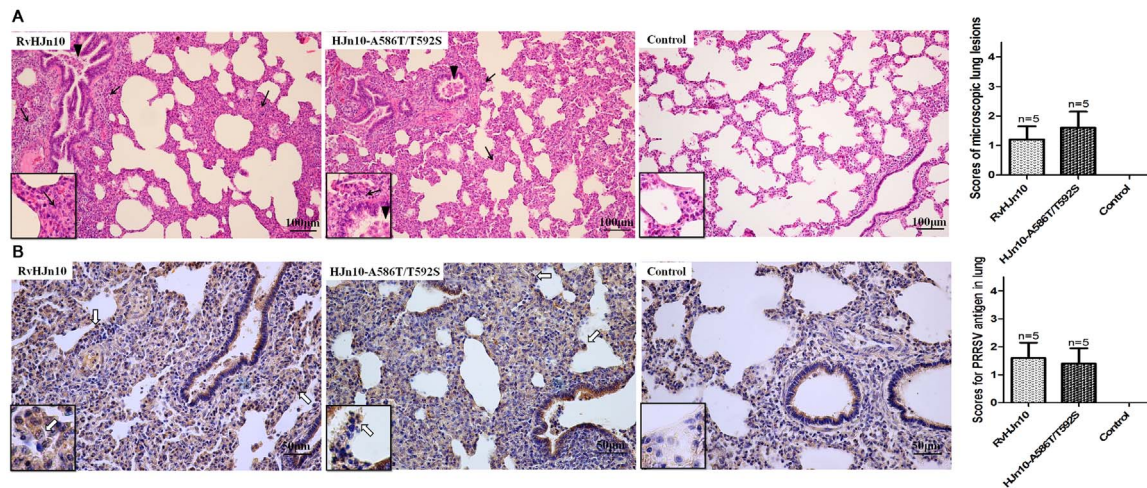


Fig. 8. Microscopic lung lesions and immunohistochemical examination for PRRSV antigen in lungs of piglets inoculated with RvHJn10 and HJn10- A586T/T592S. Shown are the representative microscopic lung lesions and the microscopic lesion scores by staining with hematoxylin and eosin (H&E) (A), and the representative views of immunohistochemistry and mean scores of lungs for PRRSV antigen (B).

present study. Our analyses showed that the mutation of Thr to Ala in 586 and Ser to Thr in 592 of RvHJn9n10 nsp9 led to the decreased replication efficiency of the virus, while the mutation of respective amino acid sites of RvJHn9n10 could not result in the increased replication efficiency of the virus. Then we continued to conduct the mutation of these two sites using the infectious cDNA clones of RvJXwn06 or RvJHn10, and confirmed the influences of these two residues mutation for replication efficiency. The data indicated that the respective mutations decreased the replication efficiency and viral RNA synthesis efficiency of the viruses based on RvJXwn and RvJHn10. These results together suggest that the residues in 586 and 592 of nsp9 are the key sites contributing to the replication efficiency of the Chinese HP-PRRSV, but are insufficient to determine the replication efficiency of PRRSV in general.

Animal trials data of serial mutant viruses based on the infectious cDNA clones of RvJXwn and RvJHn10 indicated that the mutation in 586 and 592 of nsp9 could lead to the decreased virulence of the viruses RvJXwn and RvJHn10 for piglets, while the mutation of these two residues in nsp9 based on the chimeric infectious clone of RvHJn10 could not enhance the pathogenicity of the virus RvHJn10 for piglets. In terms of our data, we suggest that the residues in 586 and 592 of nsp9 are critical sites natively conferring the fatal virulence of the Chinese HP-PRRSV for piglets.

Our present study further proved that the replication efficiency of PRRSV is closely related to its pathogenicity or virulence, and the nsp9 can be considered the key replicase directing the replication of PRRSV in host cells and *in vivo*. To date, the crystal structure of PRRSV nsp9 remains unknown. By using sequence alignments and homology modeling prediction with equine arterivirus (EAV) and coronavirus, the RdRp domain of PRRSV contains at least six canonical conserved motifs (A to F) (Beerens et al., 2007; Poch et al., 1989; te Velthuis, 2014). By amino acid alignment analysis of nsp9 between HP-PRRSV JXwn06 and LP-PRRSV HB-1/3.9, it is found that the differential amino acid in 427 is located between motif F and A, while other three differential amino acids is situated in motif E. Our results revealed that the Thr in 586 and Ser in 592 of HP-PRRSV nsp9 are selected to affect its replication efficiency and pathogenicity, but it is difficult to explain how these amino acids impact the feature of nsp9 due to unknown function of these motifs. What makes us more frustrated is that it is difficult to assess the RdRp activity of nsp9 because of its weak and controversial activity *in vitro* (Lehmann et al., 2016). Comparative analysis of nsp9 amino acid sequence showed that the amino acid in 586 is a conserved residue in all strains of HP-PRRSV, namely the amino acid in 586 of nsp9 is Thr in HP-PRRSV, whereas Ala in LP-PRRSV. However, the amino acid in 592

is Thr only in HB-1/3.9 and its wild-type HB-1(sh)/2002 (Gao et al., 2004), whereas Ser in other strains. In addition, our animal trails indicated that the amino acid in 586 impacted more obviously the virus pathogenicity than the amino acid in 592. Thus, it is proposed that the amino acid in 586 of nsp9 shares common feature affecting the replication efficiency and pathogenicity of PRRSV, while the effect of the amino acid in 592 on viral replication efficiency and pathogenicity might be strain-specific. Another concern is that, by mutating these two amino acid sites, the virulence of HP-PRRSV JXwn06 could be attenuated, whereas the replication efficiency and pathogenicity of LP-PRRSV HB-1/3.9 could not be enhanced reversely. These findings imply that other unknown factors may participate in this influence for the pathogenicity of PRRSV although the two amino acids in 586 and 592 of nsp9 are recognized as critical sites conferring the fatal virulence of HP-PRRSV in the current study. One example is that HP-PRRSV can be attenuated by de-optimization of codon pair bias in nsp9-coding region without any amino acid changes (Gao et al., 2015).

Many host cellular factors have been proved to interact with nsp9 and regulate the replication or RNA synthesis of PRRSV (Dong et al., 2014; Li et al., 2014a; Liu et al., 2016; Zhao et al., 2015). In another aspect, our results also suggested that the virulence of mutant viruses could be more remarkable decreased by the nsp10 of HB-1/3.9, although the replication efficiency changes were not observed. Previous studies have demonstrated that some nonstructural proteins of nidovirus can interact with each other, and indicated that the polymerase and helicase can interact with each other *in vitro* (von Brunn et al., 2007). We propose that there are two possible mechanisms of affecting virus replication efficiency and pathogenicity by mutating these two amino acids: they might directly affect the normal function of viral RNA amplification, or impact the interaction between nsp9 and host factors or other viral proteins. These are required to be further investigated in the future work.

As a whole, our findings indicate that the amino acids in 586 and 592 of nsp9 contribute to the replication efficiency of the Chinese HP-PRRSV in PAMs, and are critical sites natively in determining its fatal virulence for piglets, providing essential evidence for understanding the molecular basis in relation to the virulence of the Chinese HP-PRRSV for pigs.

Acknowledgements

This study was supported by Key Project of National Natural Science Funds from National Natural Science Foundation of China (31330077) and National Key Basic Research Plan Grant from the Chinese Ministry

of Science and Technology (2014CB542700), and the earmarked fund for China Agriculture Research System from the Chinese Ministry of Agriculture (CARS-35).

References

- Albina, E., 1997. Epidemiology of porcine reproductive and respiratory syndrome (PRRS): an overview. *Vet. Microbiol.* 55, 309–316.
- Allende, R., Lewis, T.L., Lu, Z., Rock, D.L., Kutish, G.F., Ali, A., Doster, A.R., Osorio, F.A., 1999. North American and European porcine reproductive and respiratory syndrome viruses differ in non-structural protein coding regions. *J. Gen. Virol.* 80 (Pt 2), 307–315.
- Benfield, D.A., Nelson, E., Collins, J.E., Harris, L., Goyal, S.M., Robison, D., Christianson, W.T., Morrison, R.B., Gorcyca, D., Chladek, D., 1992. Characterization of swine infertility and respiratory syndrome (SIRS) virus (isolate ATCC VR-2332). *J. Vet. Diagn. Invest.* 1992 (4), 127–133.
- Beerens, N., Selisko, B., Ricagno, S., Imbert, I., van der Zanden, L., Snijder, E.J., Canard, B., 2007. De novo initiation of RNA synthesis by the arterivirus RNA-dependent RNA polymerase. *J. Virol.* 81, 8384–8395.
- Brault, A.C., Huang, C.Y., Langevin, S.A., Kinney, R.M., Bowen, R.A., Ramey, W.N., Panella, N.A., Holmes, E.C., Powers, A.M., Miller, B.R., 2007. A single positively selected West Nile viral mutation confers increased virogenesis in American crows. *Nat. Genet.* 39, 1162–1166.
- Deng, Z., Lehmann, K.C., Li, X., Feng, C., Wang, G., Zhang, Q., Qi, X., Yu, L., Zhang, X., Feng, W., Wu, W., Gong, P., Tao, Y., Posthuma, C.C., Snijder, E.J., Gorbalenya, A.E., Chen, Z., 2014. Structural basis for the regulatory function of a complex zinc-binding domain in a replicative arterivirus helicase resembling a nonsense-mediated mRNA decay helicase. *Nucleic Acids Res.* 42, 3464–3477.
- Dong, J., Zhang, N., Ge, X., Zhou, L., Guo, X., Yang, H., 2014. The interaction of non-structural protein 9 with retinoblastoma protein benefits the replication of genotype 2 porcine reproductive and respiratory syndrome virus in vitro. *Virology* 464–465, 432–440.
- Fang, Y., Snijder, E.J., 2010. The PRRSV replicase: exploring the multifunctionality of an intriguing set of nonstructural proteins. *Virus Res.* 154, 61–76.
- Fang, Y., Treffers, E.E., Li, Y., Tas, A., Sun, Z., van der Meer, Y., de Ru, A.H., van Veelen, P.A., Atkins, J.F., Snijder, E.J., Firth, A.E., 2012. Efficient-2 frameshifting by mammalian ribosomes to synthesize an additional arterivirus protein. *Proc. Natl. Acad. Sci. USA* 109, E2920–E2928.
- Gao, L., Wang, L., Huang, C., Yang, L., Guo, X.K., Yu, Z., Liu, Y., Yang, P., Feng, W.H., 2015. HP-PRRSV is attenuated by de-optimization of codon pair bias in its RNA-dependent RNA polymerase nsp9 gene. *Virology* 485, 135–144.
- Gao, Z.Q., Guo, X., Yang, H.C., 2004. Genomic characterization of two Chinese isolates of porcine reproductive and respiratory syndrome virus. *Arch. Virol.* 149, 1341–1351.
- Gorbalenya, A.E., Koonin, E.V., Donchenko, A.P., Blinov, V.M., 1989. Coronavirus genome: prediction of putative functional domains in the non-structural polyprotein by comparative amino acid sequence analysis. *Nucleic Acids Res.* 17, 4847–4861.
- Guo, B., Lager, K.M., Henningson, J.N., Miller, L.C., Schlink, S.N., Kappes, M.A., Kehrl, Jr., M.E., Brockmeier, S.L., Nicholson, T.L., Yang, H.C., Faaberg, K.S., 2013. Experimental infection of United States swine with a Chinese highly pathogenic strain of porcine reproductive and respiratory syndrome virus. *Virology* 435, 372–384.
- Halbur, P.G., Paul, P.S., Frey, M.L., Landgraf, J., Eernisse, K., Meng, X.J., Lum, M.A., Andrews, J.J., Rathje, J.A., 1995. Comparison of the pathogenicity of two US porcine reproductive and respiratory syndrome virus isolates with that of the Lelystad virus. *Vet. Pathol.* 32, 648–660.
- Halbur, P.G., Paul, P.S., Frey, M.L., Landgraf, J., Eernisse, K., Meng, X.J., Andrews, J.J., Lum, M.A., Rathje, J.A., 1996. Comparison of the antigen distribution of two US porcine reproductive and respiratory syndrome virus isolates with that of the Lelystad virus. *Vet. Pathol.* 33, 159–170.
- Han, D., Hu, Y., Li, L., Tian, H., Chen, Z., Wang, L., Ma, H., Yang, H., Teng, K., 2014. Highly pathogenic porcine reproductive and respiratory syndrome virus infection results in acute lung injury of the infected pigs. *Vet. Microbiol.* 169, 135–146.
- Han, J., Wang, Y., Faaberg, K.S., 2006. Complete genome analysis of RFLP 184 isolates of porcine reproductive and respiratory syndrome virus. *Virus Res.* 122, 175–182.
- Han, J., Zhou, L., Ge, X., Guo, X., Yang, H., 2017. Pathogenesis and control of the Chinese highly pathogenic porcine reproductive and respiratory syndrome virus. *Vet. Microbiol.* 209, 30–47.
- Hanley, K.A., Lee, J.J., Blaney Jr., J.E., Murphy, B.R., Whitehead, S.S., 2002. Paired charge-to-alanine mutagenesis of dengue virus type 4 NS5 generates mutants with temperature-sensitive, host range, and mouse attenuation phenotypes. *J. Virol.* 76, 525–531.
- He, Y., Wang, G., Liu, Y., Shi, W., Han, Z., Wu, J., Jiang, C., Wang, S., Hu, S., Wen, H., Dong, J., Liu, H., Cai, X., 2012. Characterization of thymus atrophy in piglets infected with highly pathogenic porcine reproductive and respiratory syndrome virus. *Vet. Microbiol.* 160, 455–462.
- Hu, S.P., Zhang, Z., Liu, Y.G., Tian, Z.J., Wu, D.L., Cai, X.H., He, X.J., 2013. Pathogenicity and distribution of highly pathogenic porcine reproductive and respiratory syndrome virus in pigs. *Transbound. Emerg. Dis.* 60, 351–359.
- Johnson, C.R., Griggs, T.F., Gnanandarajah, J., Murtaugh, M.P., 2011. Novel structural protein in porcine reproductive and respiratory syndrome virus encoded by an alternative ORF5 present in all arteriviruses. *J. Gen. Virol.* 92 (Pt5), 1107–1116.
- Karniychuk, U.U., Geldhof, M., Vanhee, M., Van Doorselaere, J., Saveleva, T.A., Nauwynck, H.J., 2010. Pathogenesis and antigenic characterization of a new East European subtype 3 porcine reproductive and respiratory syndrome virus isolate. *BMC Vet. Res.* 6, 30–39.
- Kuhn, J.H., Lauck, M., Bailey, A.L., Shchetinin, A.M., Vishnevskaya, T.V., Bao, Y., Ng, T., F., L., M., Schneider, B.S., Gillis, A., Tamoufe, U., Dikko, J.E., D., Takuo, J.M., Kondov, N.O., Coffey, L.L., Wolfe, N.D., Delwart, E., Clawson, A.N., Postnikova, E., Bollinger, L., Lackemeyer, M.G., Radoshitzky, S.R., Palacios, G., Wada, J., Shevtsova, Z.V., Jahrling, P.B., Lapin, B.A., Deriabin, P.G., Dunowska, M., Alkhovsky, S.V., Rogers, J., Friedrich, T.C., O'Connor, D.H., Goldberg, T.L., 2016. Reorganization and expansion of the nidoviral family Arteriviridae. *Arch. Virol.* 161, 755–768.
- Lehmann, K.C., Gorbalenya, A.E., Snijder, E.J., Posthuma, C.C., 2016. Arterivirus RNA-dependent RNA polymerase: vital enzymatic activity remains elusive. *Virology* 487, 68–74.
- Lehmann, K.C., Gulyaeva, A., Zevenhoven-Dobbe, J.C., Janssen, G.M., Ruben, M., Overkleeft, H.S., van Veelen, P.A., Samborskiy, D.V., Kravchenko, A.A., Leontovich, A.M., Sidorov, I.A., Snijder, E.J., Posthuma, C.C., Gorbalenya, A.E., 2015a. Discovery of an essential nucleotidylating activity associated with a newly delineated conserved domain in the RNA polymerase-containing protein of all nidoviruses. *Nucleic Acids Res.* 43, 8416–8434.
- Lehmann, K.C., Snijder, E.J., Posthuma, C.C., Gorbalenya, A.E., 2015b. What we know but do not understand about nidovirus helicases. *Virus Res.* 202, 12–32.
- Li, J., Guo, D., Huang, L., Yin, M., Liu, Q., Wang, Y., Yang, C., Liu, Y., Zhang, L., Tian, Z., Cai, X., Yu, L., Weng, C., 2014a. The interaction between host Annexin A2 and viral Nsp9 is beneficial for replication of porcine reproductive and respiratory syndrome virus. *Virus Res.* 189, 106–113.
- Li, L., Zhao, Q., Ge, X., Teng, K., Kuang, Y., Chen, Y., Guo, X., Yang, H., 2012. Chinese highly pathogenic porcine reproductive and respiratory syndrome virus exhibits more extensive tissue tropism for pigs. *Virol. J.* 9, 203–208.
- Li, Y., Tas, A., Sun, Z., Snijder, E.J., Fang, Y., 2015. Proteolytic processing of the porcine reproductive and respiratory syndrome virus replicase. *Virus Res.* 202, 48–59.
- Li, Y., Wang, G., Liu, Y., Tu, Y., He, Y., Wang, Z., Han, Z., Li, L., Li, A., Tao, Y., Cai, X., 2014a. Identification of apoptotic cells in the thymus of piglets infected with highly pathogenic porcine reproductive and respiratory syndrome virus. *Virus Res.* 189, 29–33.
- Li, Y., Zhou, L., Zhang, J., Ge, X., Zhou, R., Zheng, H., Geng, G., Guo, X., Yang, H., 2014b. Nsp9 and Nsp10 contribute to the fatal virulence of highly pathogenic porcine reproductive and respiratory syndrome virus emerging in China. *PLoS Pathog.* 10, e1004216.
- Liu, L., Tian, J., Nan, H., Tian, M., Li, Y., Xu, X., Huang, B., Zhou, E., Hiscox, J.A., Chen, H., 2016. Porcine reproductive and respiratory syndrome virus nucleocapsid protein interacts with Nsp9 and cellular DHX9 to regulate viral RNA synthesis. *J. Virol.* 90, 5384–5398.
- Lunney, J.K., Fang, Y., Ladinig, A., Chen, N., Li, Y., Rowland, B., Renukaradhya, G.J., 2016. Porcine reproductive and respiratory syndrome virus (PRRSV): pathogenesis and interaction with the immune system. *Annu. Rev. Anim. Biosci.* 4, 129–154.
- Mardassi, H., Mounir, S., Dea, S., 1994. Identification of major differences in the nucleocapsid protein genes of a Quebec strain and European strains of porcine reproductive and respiratory syndrome virus. *J. Gen. Virol.* 75 (Pt3), 681–685.
- Mardassi, H., Mounir, S., Dea, S., 1995. Molecular analysis of the ORFs 3 to 7 of porcine reproductive and respiratory syndrome virus, Quebec reference strain. *Arch. Virol.* 140, 1405–1418.
- Meng, X.J., Paul, P., Halbur, P., Lum, M., 1995. Phylogenetic analyses of the putative M (ORF6) and N (ORF7) genes of porcine reproductive and respiratory syndrome virus (PRRSV): implication for the existence of two genotypes of PRRSV in the USA and Europe. *Arch. Virol.* 140, 745–755.
- Meulenberg, J.J., Petersen-den Besten, A., De Kluyver, E.P., Moormann, R.J., Schaaper, W.M., Wensvoort, G., 1995. Characterization of proteins encoded by ORFs 2 to 7 of Lelystad virus. *Virology* 206, 155–163.
- Murtaugh, M.P., Elam, M.R., Kakach, L.T., 1995. Comparison of the structural protein coding sequence of the VR-2332 and Lelystad virus strain of the PRRS virus. *Arch. Virol.* 140, 1451–1460.
- Nelsen, C.J., Murtaugh, M.P., Faaberg, K.S., 1999. Porcine reproductive and respiratory syndrome virus comparison: divergent evolution on two continents. *J. Virol.* 73, 270–280.
- Poch, O., Sauvaget, I., Delarue, M., Tordo, N., 1989. Identification of four conserved motifs among the RNA-dependent polymerase encoding elements. *EMBO J.* 8, 3867–3874.
- Rosow, K.D., 1998. Porcine reproductive and respiratory syndrome. *Vet. Pathol.* 35, 1–20.
- Shi, M., Lam, T.T., Hon, C.C., Hui, R.K., Faaberg, K.S., Wennblom, T., Murtaugh, M.P., Stadeljek, T., Leung, F.C., 2010. Molecular epidemiology of PRRSV: a phylogenetic perspective. *Virus Res.* 154, 7–17.
- Snijder, E.J., den Boon, J.A., Bredenbeek, P.J., Horzinek, M.C., Rijnbrand, R., Spaan, W.J., 1990. The carboxyl-terminal part of the putative Berne virus polymerase is expressed by ribosomal frameshifting and contains sequence motifs which indicate that toro- and coronaviruses are evolutionarily related. *Nucleic Acids Res.* 18, 4535–4542.
- Spear, A., Faaberg, K.S., 2015. Development of a genome copy specific RT-qPCR assay for divergent strains of type 2 porcine reproductive and respiratory syndrome virus. *J. Virol. Methods* 218, 1–6.
- Subissi, L., Posthuma, C.C., Collet, A., Zevenhoven-Dobbe, J.C., Gorbalenya, A.E., Decroly, E., Snijder, E.J., Canard, B., Imbert, I., 2014. One severe acute respiratory syndrome coronavirus protein complex integrates processive RNA polymerase and exonuclease activities. *Proc. Natl. Acad. Sci. USA* 111, E3900–E3909.
- te Velthuis, A.J., 2014. Common and unique features of viral RNA-dependent polymerases. *Cell. Mol. Life Sci.* 71, 4403–4420.
- Tian, K., Yu, X., Zhao, T., Feng, Y., Cao, Z., Wang, C., Hu, Y., Chen, X., Hu, D., Tian, X., Liu, D., Zhang, S., Deng, X., Ding, Y., Yang, L., Zhang, Y., Xiao, H., Qiao, M., Wang, B., Hou, L., Wang, X., Yang, X., Kang, L., Sun, M., Jin, P., Wang, S., Kitamura, Y., Yan, J., Gao, G.F., 2007. Emergence of fatal PRRSV variants: unparalleled outbreaks of

- atypical PRRS in China and molecular dissection of the unique hallmark. *PLoS One* 2, e526.
- van Dinten, L.C., van Tol, H., Gorbalenya, A.E., Snijder, E.J., 2000. The predicted metal-binding region of the arterivirus helicase protein is involved in subgenomic mRNA synthesis, genome replication, and virion biogenesis. *J. Virol.* 74, 5213–5223.
- van Nieuwstadt, A.P., Meulenbergh, J.J., van Essen-Zanbergen, A., Petersen-den Besten, A., Bende, R.J., Moormann, R.J., Wensvoort, G., 1996. Proteins encoded by open reading frames 3 and 4 of the genome of Lelystad virus (Arteriviridae) are structural proteins of the virion. *J. Virol.* 70, 4767–4772.
- von Brunn, A., Teepe, C., Simpson, J.C., Pepperkok, R., Friedel, C.C., Zimmer, R., Roberts, R., Baric, R., Haas, J., 2007. Analysis of intraviral protein-protein interactions of the SARS coronavirus ORF6. *PLoS One* 2, e459.
- Wang, X., Marthaler, D., Rovira, A., Rossow, S., Murtaugh, M.P., 2015. Emergence of a virulent porcine reproductive and respiratory syndrome virus in vaccinated herds in the United States. *Virus Res.* 210, 34–41.
- Watanabe, T., Watanabe, S., Shinya, K., Kim, J.H., Hatta, M., Kawaoka, Y., 2009. Viral RNA polymerase complex promotes optimal growth of 1918 virus in the lower respiratory tract of ferrets. *Proc. Natl. Acad. Sci. USA* 106, 588–592.
- Wensvoort, G., Terpstra, C., Pol, J.M., ter Laak, E.A., Bloemraad, M., de Kluyver, E.P., Kragten, C., van Buiten, L., den Besten, A., Wagenaar, F., et al., 1991. Mystery swine disease in The Netherlands: the isolation of Lelystad virus. *Vet. Q.* 13, 121–130.
- Wu, W.H., Fang, Y., Farwell, R., Steffen-Bien, M., Rowland, R.R., Christopher-Hennings, J., Nelson, E.A., 2001. A 10-kDa structural protein of porcine reproductive and respiratory syndrome virus encoded by ORF2b. *Virology* 287, 183–191.
- Xu, X., Liu, Y., Weiss, S., Arnold, E., Sarafianos, S.G., Ding, J., 2003. Molecular model of SARS coronavirus polymerase: implications for biochemical functions and drug design. *Nucleic Acids Res.* 31, 7117–7130.
- Yoo, D., Song, C., Sun, Y., Du, Y., Kim, O., Liu, H.C., 2010. Modulation of host cell responses and evasion strategies for porcine reproductive and respiratory syndrome virus. *Virus Res.* 154, 48–60.
- Zhang, H., Guo, X., Ge, X., Chen, Y., Sun, Q., Yang, H., 2009. Changes in the cellular proteins of pulmonary alveolar macrophage infected with porcine reproductive and respiratory syndrome virus by proteomics analysis. *J. Proteome Res.* 8, 3091–3097.
- Zhao, S., Ge, X., Wang, X., Liu, A., Guo, X., Zhou, L., Yu, K., Yang, H., 2015. The DEAD-box RNA helicase 5 positively regulates the replication of porcine reproductive and respiratory syndrome virus by interacting with viral Nsp9 in vitro. *Virus Res.* 195, 217–224.
- Zhou, L., Wang, Z., Ding, Y., Ge, X., Guo, X., Yang, H., 2015. NADC30-like strain of porcine reproductive and respiratory syndrome virus, China. *Emerg. Infect. Dis.* 21, 2256–2257.
- Zhou, L., Yang, H., 2010. Porcine reproductive and respiratory syndrome in China. *Virus Res.* 154, 31–37.
- Zhou, L., Zhang, J., Zeng, J., Yin, S., Li, Y., Zheng, L., Guo, X., Ge, X., Yang, H., 2009. The 30-amino-acid deletion in the Nsp2 of highly pathogenic porcine reproductive and respiratory syndrome virus emerging in China is not related to its virulence. *J. Virol.* 83, 5156–5167.